

Supporting Information

Arsenic in Lake Geneva (Switzerland, France): long term monitoring, and redox and  
methylation speciation in an As unpolluted, oligo-mesotrophic lake

Montserrat Filella<sup>a</sup>, Sebastian Wey<sup>a</sup>, Tomáš Matoušek<sup>b</sup>, Mathieu Coster<sup>c</sup>, Juan-Carlos Rodríguez-  
Murillo<sup>d</sup>, Jean-Luc Loizeau<sup>a</sup>

<sup>a</sup>Department F.-A. Forel for environmental and aquatic sciences, University of Geneva,  
Boulevard Carl-Vogt 66, CH-1205 Geneva, Switzerland

<sup>b</sup>Institute of Analytical Chemistry of the Czech Academy of Sciences, Veveří 97, 602 00 Brno,  
Czech Republic

<sup>c</sup>Service de l'écologie de l'Eau, Geneva, Switzerland

<sup>d</sup>Museo Nacional de Ciencias Naturales, CSIC, Serrano 115 dpdo, E-28006 Madrid, Spain

## CONTENTS

Section SI1. Details on the analysis of arsenic species.

Section SI2. Detailed description of arsenic species profiles.

Table SI1. Names, abbreviations, and structures of arsenic species in aqueous media.

Table SI2. Lake Geneva watershed main features.

Table SI3. Main tributaries of Lake Geneva.

Table SI4. River sampling points.

Table SI5. HG and ICP-MS/MS settings.

Table SI6. Results of CRM SLRS-6 obtained in the analysis of individual batches.

Table SI7.  $As_{tot,dis}$  concentrations ( $\mu\text{g L}^{-1}$ ) at 10 depths and 6 sampling dates at GE3.

Table SI8. Sum of the concentrations of all investigated As species (sumAs) ( $\mu\text{g L}^{-1}$ ) at 10 depths and 6 sampling dates at GE3.

Table SI9.  $As_{tot,dis}$  concentrations ( $\mu\text{g L}^{-1}$ ) at two sampling dates and 11 and 13 depths, respectively, at SHL2.

Table SI10. Sum of the concentrations of all investigated As species (sumAs) ( $\mu\text{g L}^{-1}$ ) at two sampling dates and 11 and 13 depths, respectively, at SHL2.

Table SI11.  $As_{tot,dis}$  and sumAs concentrations ( $\mu\text{g L}^{-1}$ ) in three sediment cores (C1, C2, C3).

Table SI12.  $iAs(III+V)$  and  $iAs(III)$  concentrations ( $\text{ng L}^{-1}$ ) determined by HG-CT-ICP-MS at 10 depths and 6 sampling dates at GE3.

Table SI13.  $MA(III+V)$ ,  $DMA(III+V)$  and TMAO concentrations ( $\text{ng L}^{-1}$ ) determined by HG-CT-ICP-MS at 10 depths and 6 sampling dates at GE3.

Table SI14.  $iAs(III+V)$ ,  $iAs(III)$ ,  $MA(III+V)$ ,  $DMA(III+V)$  and TMAO concentrations ( $\text{ng L}^{-1}$ ) determined by HG-CT-ICP-MS at two sampling dates and 11 and 13 depths, respectively, at SHL2.

Table SI15.  $iAs(III+V)$ ,  $iAs(III)$ ,  $MA(III+V)$ ,  $DMA(III+V)$  and TMAO concentrations ( $\text{ng L}^{-1}$ ) in three sediment cores (C1, C2, C3).

Table SI16a. Seasonality analysis. Results of Kruskal-Wallis test ( $p$  values) for each period and all data normalised.

Table SI16b. Seasonality analysis. Results of Kruskal-Wallis test ( $p$  values) for each period and all data normalised.

Table SI7a. Temporal trend analysis. Results of the seasonal Mann-Kendall test (SMK) for each period and all data normalised.

Table SI7b. Temporal trend analysis. Results of the seasonal Mann-Kendall test (SMK) for each period and all data normalised.

Figure SI1. Water discharge of the River Rhone at « Porte-du-Scex ». Values cover the period 1935–2021.

Figure SI2. Pore water sampling using Rhizon Core Solution Sampler.

Figure SI3. Monthly specific As mass inventories of  $A_{Stot,dis}$  from 2015 to 2021.

Figure SI4. Fourier power spectra (REDFIT) of normalized total ‘dissolved’ As concentrations at 0 and 70 m at point G3.

Figure SI5. Stability of iAs(III) species in lake water.

## Section SI1. Details on the analysis of arsenic species.

Analysis of inorganic and methylated As species was conducted following the method described in Matoušek et al. (2013)<sup>1</sup> and Filella and Matoušek (2022).<sup>2</sup> Samples were injected into the HG system without further pre-treatment, except for pre-reduction of aliquots for analysis of iAs(III+V), MA(III+V) and DMA (III+V) species. In this case, 145  $\mu\text{L}$  of a 20% L-cysteine hydrochloride monohydrate (Bio-Ultra, Sigma) solution was added to 1.45 mL of sample 1–3 hours prior to analysis. Pore water samples which showed high  $\text{As}_{\text{tot,dis}}$  concentrations were diluted before HG so that iAs(III+V) concentrations would not exceed  $2 \mu\text{g L}^{-1}$ . 500  $\mu\text{L}$  of sample rinsed with 500  $\mu\text{L}$  of water was manually pipetted into HG system for each trapping cycle. It was sequentially mixed with flows of 0.75 M Tris-HCl buffer (tris(hydroxymethyl) aminomethane hydrochloride (Trizma® hydrochloride, Sigma) adjusted to pH 6 by KOH (semiconductor grade, Sigma) and with a 1%  $\text{NaBH}_4$  (Fluka) reducing solution in 0.1% KOH. Generated volatile (methylated) hydrides were collected, preconcentrated and separated in a quartz U-tube filled with approximately 0.9 g of Chromosorb WAW-DMCS 45/60, 15 % OV-3 (Supelco). Cooling of U-tube and heating for sequential desorption of hydrides was performed in a semi-automated system on a Perkin-Elmer FIAS unit.<sup>3</sup> ICP-MS/MS Agilent 8900 in  $\text{O}_2$  mode with mass shift ( $m/z$  75->91) was used for detection. A co-nebulized solution of  $2 \mu\text{g L}^{-1}$  Y ( $m/z$  89->105) was used as an internal standard for drift correction. The complete HG-CT-ICP MS/MS parameters are shown in Table SI5.

Commercial ultratrace metal analysis water (ANALPURE® Ultra, Analytika s.r.o., Czech Republic), yielding slightly lower iAs(III) blanks ( $3\text{--}5 \text{ ng L}^{-1}$  iAs(III)), or Teflon subboil distilled deionized water (SBDIW) were used throughout for aliquots of trivalent and pre-reduced samples, respectively. Quantification was performed by external calibration using a standard containing a mix of individual species, except MA(III) which were quantified on iAs(III) calibration since the sensitivity of the method should be similar to iAs(III).<sup>4</sup>

Working mixed calibration standards were prepared daily at concentrations 1000/40/100/40  $\text{ng L}^{-1}$  As of iAs(III), MA(V), DMA(V) and TMAO (or twice these concentrations when more concentrated samples

such as SHL2 and sediment samples had to be analysed) by dilution from a mixed stock standard solution. This stock solution was prepared monthly in SBDIW water at concentrations 50/2/5/2  $\mu\text{g L}^{-1}$  As of iAs(III), MA(V), DMA(V) and TMAO from single species standards of 10  $\text{mg L}^{-1}$  iAs(III) (prepared from  $\text{As}_2\text{O}_3$ , Lachema, Czech Rep.) and 100  $\mu\text{g L}^{-1}$  of MA(V) (methylarsonic acid, disodium salt ( $\text{CH}_3\text{AsO}(\text{ONa})_2$ ), Chem Service, West Chester, PA), DMA(V) (dimethylarsinic acid ( $(\text{CH}_3)_2\text{AsO}(\text{OH})$ ) Chem Service, West Chester, PA) and TMAO (trimethylarsine oxide,  $(\text{CH}_3)_3\text{AsO}$ , courtesy of W. Cullen, University of British Columbia). Single species solutions were standardized by GF AAS for As content and checked for species purity by HPLC-ICP-MS/MS.

Samples were analysed using two replicates per sample. Concentrations given are the average values of the replicates. The data in-day precision was estimated as the uncertainty within a single profile, assessed as the relative standard deviation (RSD) of all replicates of all January 2021 or February 2021 samples (assuming that the lake was well mixed and concentration identical, see below) and it was better than 2% for all species ( $n=10$ ) except 3.1% for DMA(III+V) (3.1% at 11  $\text{ng L}^{-1}$ ) and MA(III) (below LOD). The inter-day uncertainty, i.e. comparison between values of individual profiles, could be assessed in similar manner from values of CRM SLRS-6 analysed with each profile. In this case, the RSD was better than 4% ( $n=9$ ) except for TMAO (11% at 18  $\text{ng L}^{-1}$ ) (Table SI6). The mean values of SLRS-6 analyses were in good agreement with information values provided in the accompanying certificate (88-112%, Table SI6), and the sum of species (mean  $507 \pm 15 \text{ ng L}^{-1}$  As) agreed well with certified total As content ( $570 \pm 80 \text{ ng L}^{-1}$  As) and the sum of information values of species (521  $\text{ng L}^{-1}$  As). It should be mentioned, however, that information values of species in this CRM were based mainly on data obtained by the same analytical method and laboratory.

#### *Sample stability testing*

Tests on species stability and conservation were performed in January 2021, before the first lake sampling campaign. The preservation of unfiltered or filtered samples (0.20  $\mu\text{m}$ ) stabilized by addition of either 2

mM EDTA or HNO<sub>3</sub> to pH 1, and stored at 4°C was evaluated by repeated analyses. Three aliquots of each treatment were analysed, with a spare fourth aliquot opened and analysed after 156 days.

The concentrations of iAs(III+V), MA(III+V) DMA(III+V) and TMAO remained reasonably stable for 3–4 months, with acid conserved samples yielding approx. 10–15% lower values than the EDTA conserved ones at the end of the testing period (Figure SI5). Freshly opened aliquots after 156 days yielded similar values as initial aliquots. Since the main concern was the oxidation state stability of iAs(III), another set of aliquots was spiked with 500 ng L<sup>-1</sup> iAs(III) one day after sampling. Results are shown in Figure SI5. After 11 days, unfiltered samples showed a substantial increase of iAs (III) concentrations while filtered but unpreserved samples showed ~20% oxidation. Filtered and preserved samples had good iAs(III) stability both at the natural level, i.e. 27 ng L<sup>-1</sup> iAs(III) or spiked samples over at least 120 days. It can be concluded that both methods are suitable for conservation, at least for the two-week period during which the samples were analysed in this study. Notably, acidified samples showed higher presence of iAs(III) than the other treatments (45 ng L<sup>-1</sup> compared to 23–27 ng L<sup>-1</sup> iAs(III)). This was not due to acid blank, but an artefact caused by limited selectivity: acidification interferes with the pH-selectivity principle of oxidation state specific HG, generating a small signal of “apparent” iAs(III) in presence of approximately 800 ng L<sup>-1</sup> iAs(V). The EDTA conservation was preferred because of slightly better performance and no selectivity issues and was used throughout further work.

The stability of MA(III) in the samples could not be properly verified because MA(III) was not present in the January testing samples. A repeated analysis of two March samples, after 27 days, still yielded approximately half of observed MA(III), suggesting a reasonable stability over the three days between sampling and analysis (with the exception of 10 days for March samples).

## Section SI2. Detailed description of arsenic species profiles.

### *Petit Lac*

Concentrations of iAs(V) were fairly constant with depth in January, February and March (Table SI12 and Figure 6). The decrease observed for  $As_{tot,dis}$  in March was also clearly observed in iAs(V) concentrations (i.e.,  $651 \text{ ng L}^{-1}$  in March compared to  $817 \text{ ng L}^{-1}$  in February). Concentrations of iAs(V) in surface water were depleted in the profiles of April, May and June, with minimum values at 7.5 m (April, May) and 2.5 m (June). iAs(V) concentrations increased with depth and reached values similar to those observed in winter. Concentrations of iAs(III) (Table SI12 and Figure 6) were distributed evenly across depth in January, February and March, with mean concentrations in January ( $22.9 \text{ ng L}^{-1}$ ) and February ( $24.4 \text{ ng L}^{-1}$ ) lower than in March ( $65.7 \text{ ng L}^{-1}$ ). A drastic increase in iAs(III) concentrations in surface waters was observed between March and April when concentrations in the first 10 m were clearly above  $300 \text{ ng L}^{-1}$ . Concentrations of iAs(III) in May in surface waters were still above those observed during the winter months, decreasing with depth to  $31 \text{ ng L}^{-1}$  (65 m), close to concentrations observed in winter. In May and June, concentrations at the bottom of the lake were relatively similar and generally low, but after the drop observed in May, iAs(III) concentrations rose in surface waters in June.

Concentrations of MA(III+V) were lower than those of other As species (Table SI13 and Figure 6). They were constant across depth from January to April. Differences in MA(III+V) concentrations across the first three months were all significant (pairwise Wilcoxon test,  $p < 0.001$ ). Between March and April, an increase in concentrations of MA(III+V) could be observed, also significant (Wilcoxon test,  $p < 0.001$ ). A clear increase in concentrations in the epilimnion in May ( $20 \text{ ng L}^{-1}$ ) and June was observed, with MA(III+V) concentrations slightly lower at the bottom of the lake than in winter.

Low but quantifiable concentrations of MA(III) were found in March to June profiles (Figure 6). While March profile was fairly uniform at about  $0.7 \text{ ng L}^{-1}$ , April profile were depleted above 15 m depth, with approximate concentrations of 0.4 and  $0.65 \text{ ng L}^{-1}$ , respectively, below 15 m. June profile had a distinctive

maximum of  $1.5 \text{ ng L}^{-1}$  at 15–20 m. It should be noted that MA(III) is unstable towards oxidation and that original concentrations may have been even slightly higher than reported (see Section SI1).

Like other As species, DMA(III+V) concentrations were uniformly distributed across depths during the first three sampling dates (Table SI13 and Figure 6). Similar to the behaviour of iAs(III), overall DMA(III+V) concentrations were increasing between February and March. Concentrations in surface water in April were around  $100 \text{ ng L}^{-1}$  but decreased towards the bottom of the lake, reaching a minimum of  $73 \text{ ng L}^{-1}$  at 65 m. Similar to concentrations of iAs(III), but in contrast to MA(III+V), DMA(III+V) concentrations dropped across the whole profile between April and May. The highest concentrations of DMA(III+V) were reached in June with the highest value directly below the lake's surface, which marks a contrast to the profile of iAs(III). In June, DMA(III+V) concentration decreased to concentrations as low as  $24 \text{ ng L}^{-1}$  at 65 m. No detectable concentrations of DMA(III) were found in any profile, either because it was not present, or due to its tendency to fast oxidation.

TMAO concentrations were low and they showed similarities with the profiles of other As species (Table SI13 and Figure 6). Whereas concentrations in January, February and March were constant across depth, they were generally higher in surface waters than in greater depths in the following months. Unlike the evolution of MA(III+V), TMAO did not show a marked increase in mean concentration between March and April, surface concentrations further increased in May and June, showing maximum values at 5 m. Concentrations in the deeper water layers decreased as the year progressed.

### *Grand Lac*

Figure 7 (and Table SI14) shows that the increase in iAs(V) concentrations starting from 100 m downwards is responsible for the increase of  $A_{\text{Stot,dis}}$  with depth. Concentrations of iAs(III) were close to zero below a depth of 50 m ( $9 \text{ ng L}^{-1}$  between 100 and 300 m) at both sampling dates. Constant and low concentrations of DMA(III+V) ( $15.0 \text{ ng L}^{-1}$ ) were reached at 100 m in April. Values were approaching the lowest observed concentrations closer to the surface in June, but reached similar values ( $16.5 \text{ ng L}^{-1}$  between 100 and 300

m). MA(III+V) and TMAO approached zero at greater depths than iAs(III) where DMA(III+V) approached its lowest concentration. However, their concentrations were very low and could not offset the dominance of iAs(V) in deeper parts of the lake. In April, iAs(III) concentration reached values up to 400 ng L<sup>-1</sup>. iAs(III) concentrations were generally lower in June. In addition, iAs(III) concentration peaked at 5 m in June and diminished quickly with increasing depth. This stands in contrast to the observations in April, where the maximum concentration was observed at 10 m and remained elevated within the next few metres. The same behaviour could be observed for concentrations of DMA(III+V). Even though concentrations in the first few metres were higher in June than in April and reached values up to 175 ng L<sup>-1</sup> at 0 m, they decreased quickly with depth. MA(III+V) behaved similarly, but the decrease took place at a slower rate.

Table SII. Names, abbreviations, and structures of arsenic species in aqueous media. The species are drawn in their most deprotonated form. Adapted from Francesconi and Kuehnelt (2004).<sup>4</sup>

Arsenite, iAs(III)	Arsenate, iAs(V)	Methylarsonite, MA(III)
$\begin{array}{c} \text{OH} \\   \\ \text{HO} - \text{As} \\   \\ \text{OH} \end{array}$	$\begin{array}{c} \text{OH} \\   \\ \text{HO} - \text{As} = \text{O} \\   \\ \text{OH} \end{array}$	$\begin{array}{c} \text{CH}_3 \\   \\ \text{HO} - \text{As} \\   \\ \text{OH} \end{array}$
Methylarsonate, MA(V)	Dimethylarsinite, DMA(III)	Dimethylarsinate, DMA(V)
$\begin{array}{c} \text{CH}_3 \\   \\ \text{HO} - \text{As} = \text{O} \\   \\ \text{OH} \end{array}$	$\begin{array}{c} \text{CH}_3 \\   \\ \text{H}_3\text{C} - \text{As} \\   \\ \text{OH} \end{array}$	$\begin{array}{c} \text{CH}_3 \\   \\ \text{H}_3\text{C} - \text{As} = \text{O} \\   \\ \text{OH} \end{array}$
Trimethylarsine oxide, TMAO	Arsenobetaine	
$\begin{array}{c} \text{CH}_3 \\   \\ \text{H}_3\text{C} - \text{As} = \text{O} \\   \\ \text{CH}_3 \end{array}$	$\begin{array}{c} \text{CH}_3 \\   \\ \text{H}_3\text{C} - \text{As}^+ - \text{CH}_2\text{COO}^- \\   \\ \text{CH}_3 \end{array}$	

Table SI2. Lake Geneva watershed main features (CIPEL 2022).<sup>5</sup>

---

Average geographical position: 46° 27' N, 6° 32' E

Average annual altitude of the body of water (1943–2021): 372.05 m

Length of banks: 200.2 km (France: 58.0 km; Switzerland: 142.2 km)

Surface of the lake: 580.1 km<sup>2</sup> (France: 234.8 km<sup>2</sup>; Switzerland: 345.3 km<sup>2</sup>)

Average volume: 89 km<sup>3</sup>

Average annual flow of the upstream Rhône (at the Porte du Scex) (1935–2021): 183 m<sup>3</sup> s<sup>-1</sup>

Average annual discharge from the Rhone to the outlet (in Geneva) (1935–2021): 250 m<sup>3</sup> s<sup>-1</sup>

Theoretical water residence time: 11.3 years

Length of its axis: 72.3 km

Maximum depth: 309.7 m

Average depth: 152.7 m

---

Surface of the catchment area (lake included): 7999 km<sup>2</sup>

Average altitude: 1670 m

Maximum altitude (Pointe Dufour): 4634 m

Glaciation index (relative to total area): 9.40 %

Permanent population: 1,400,847 (France, 2017: 168,639, Switzerland, 2018: 1,232,208)

Distribution of the most important land use patterns:

- Water surfaces: 7%
- Built: 7%
- Unproductive land: 29%
- Forests: 31%
- Cultivable land: 26% (distribution: 62% grassland, 22% arable lands, 4% vineyards, 2% arboriculture, 10% heterogeneous uses)

Wastewater treatment plants: 162 (population equivalent: 3,048,985)

---

Table SI3. Main tributaries of Lake Geneva. They are ordered counter-clockwise. Only tributaries longer than 10 km are included. Source: Wikipedia.

River	Length / km	Surface of catchment / km <sup>2</sup>	Mean discharge / m <sup>3</sup> s <sup>-1</sup> <sup>a</sup>	Elevation of source / m asl
Rhone	165	5238	183	2208
Eau Froide	11.3	23.4	0.532	1498
Veveyse	19.5	64.5	2.02	1783
Le Flon	11.5	23.0	0.669	830
Venoge	38.4	236	4.2	762
Morges	14.9	35.6	0.434	620
Aubonne	12.2	96.3	5.6	700
Promenthouse	16.0	100	1.7	971
Versoix	21.9	90.7	3.2	600
Hermance	13.0	42.5	0.140	583
Redon	11.7	30.5	0.472	875
Dranse	49.1	495	19.6	

<sup>a</sup>Values close to the river mouths; they should be considered as indicative only.

Table SI4. River sampling points. Complementary data corresponds to the closest BAFU monitoring points ([www.hydrodaten.admin.ch/](http://www.hydrodaten.admin.ch/)) for Swiss rivers, except Versoix ([www.vhg.ch](http://www.vhg.ch)) and to the Reyvroz hydrological station, 20 km upstream of the Dranse inlet to Lake Geneva in the Dranse River ([www.hydro.eaufrance.fr](http://www.hydro.eaufrance.fr)).

River	Coordinates	Elevation / m asl	Surface of catchment / km <sup>2</sup>	Mean elevation of catchment / m asl	Glaciation %
Rhone, Porte du Scex	6.8884° E/46.3492° N	377	5238	2127	11.1
Aubonne	6.4067° E/46.4767° N	390	105	952	0
Dranse	6.5076° E/46.3829° N	520	495	–	–
Venoge	6.5447° E/46.5106° N	383	228	686	0
Versoix	6.1659° E/46.2764° N	375	87.3	–	0

Table SI5. HG and ICP-MS/MS settings.

<i>HG-CT parameters</i>	
Reaction buffer	TRIS-HCl 0.75M, pH 6
Reductant	1% NaBH <sub>4</sub> in 0.1% KOH
Sample, buffer and reductant flow rate	1 mL min <sup>-1</sup> each
HG Carrier gas	He 75 mL min <sup>-1</sup>
<i>ICP-MS/MS tune parameters</i>	
RF power	1550 W
Sample depth	8mm
Carrier gas	Ar 0.6 L min <sup>-1</sup>
Dilution gas	Ar 0.6 L min <sup>-1</sup>
Nebulizer pump flow rate	0.3 mL min <sup>-1</sup>
Internal standard solution	Y 2 µg L <sup>-1</sup> + Rh 10 µg L <sup>-1</sup> in 2% HNO <sub>3</sub>
Spray chamber temperature	2 °C
Reaction Cell O <sub>2</sub> gas flow	40%
Deflect	-15 V
Axial acceleration	2 V
Energy discrimination	-7 V

Table SI6. Results of CRM SLRS-6 obtained in the analysis of individual batches.

Sample batch	[iAs(III+V)] / ng L <sup>-1</sup>	[MA(III+V)] / ng L <sup>-1</sup>	[DMA(III+V)] / ng L <sup>-1</sup>	[TMAO] / ng L <sup>-1</sup>	sumAs / ng L <sup>-1</sup>
GE3 January	351	80	76	19	526
GE3 February	342	84	79	21	525
GE3 March	334	79	74	19	507
SHL2 + rivers April	329	78	74	16	497
GE3 April	338	79	75	14	505
GE3 May	341	79	77	19	517
GE3 + rivers June	335	78	72	19	503
SHL2 June	338	76	70	19	503
Sediments	313	72	74	19	478
Mean	336	78	75	18	507
St dev	11	3	3	2	15
RSD	3%	4%	4%	11%	3%
Certificate information value	360	70	70	21	521
Certified total As					<b>570 ± 80</b>

Table SI7.  $As_{tot,dis}$  concentrations ( $\mu\text{g L}^{-1}$ ) at 10 depths and 6 sampling dates at GE3.

Depth / m	26 Jan 2021	16 Feb 2021	16 Mar 2021	20 Apr 2021	15 May 2021	22 Jun 2021
0	1.02	1.09	0.966	1.1	1.06	1.05
2.5	1.04	1.04	0.966	1.07	1.08	1.07
5	1.04	1.07	0.965	1.07	1.05	1.09
7.5	1.03	1.05	0.999	1.12	1.1	1.09
10	1.06	1.04	0.962	1.11	1.07	1.03
15	1.04	1.06	0.98	1.13	1.06	1.08
20	1.05	1.01	1.01	1.08	1.07	1.04
30	1.06	1.07	1	1.08	1.01	1.02
50	0.992	1.08	1.01	1.12	1.08	1.1
65	1.01	1.08	1.02	1.12	1.1	1.15

Table SI8. Sum of the concentrations of all investigated As species (sumAs) ( $\mu\text{g L}^{-1}$ ) at 10 depths and 6 sampling dates at GE3.

Depth / m	26 Jan 2021	16 Feb 2021	16 Mar 2021	20 Apr 2021	15 May 2021	22 Jun 2021
0	0.89	0.88	0.78	0.88	0.88	0.85
2.5	0.88	0.89	0.78	0.87	0.89	0.85
5	0.89	0.89	0.78	0.89	0.89	0.85
7.5	0.89	0.89	0.78	0.88	0.88	0.88
10	0.89	0.89	0.78	0.87	0.89	0.87
15	0.90	0.89	0.78	0.87	0.88	0.88
20	0.89	0.88	0.79	0.87	0.89	0.86
30	0.91	0.88	0.78	0.88	0.90	0.85
50	0.91	0.88	0.78	0.89	0.94	0.96
65	0.91	0.86	0.78	0.90	0.99	1.01

Table SI9.  $A_{\text{Stot,dis}}$  concentrations ( $\mu\text{g L}^{-1}$ ) at two sampling dates and 11 and 13 depths, respectively, at SHL2.

Depth / m	20 April 2021	14 June 2021
0	1.08	1.04
5	1.12	1.05
10	1.09	1.05
15	1.12	0.90
20		1.00
25		1.11
30	1.12	1.10
35	1.09	1.14
50	1.12	1.14
100	1.14	1.16
150	1.3	1.42
200	1.83	1.74
300	2.45	2.28

Table SI10. Sum of the concentrations of all investigated As species (sumAs) ( $\mu\text{g L}^{-1}$ ) at two sampling dates and 11 and 13 depths, respectively, at SHL2.

Depth / m	20 April 2021	14 June 2021
0	0.87	0.84
5	0.86	0.85
10	0.85	0.84
15	0.85	0.72
20		0.80
25		0.90
30	0.86	0.89
35	0.87	0.94
50	0.91	0.95
100	0.93	0.98
150	1.17	1.26
200	1.48	1.53
300	1.98	2.03

Table SI11.  $A_{\text{tot,dis}}$  and sumAs concentrations ( $\mu\text{g L}^{-1}$ ) in three sediment cores (C1, C2, C3). See text for location. SN: supernatant, S1: 1 cm, S2: 4 cm, S3: 7 cm under the sediment-water interface, 12 July 2021.

	C1		C2		C3	
	$A_{\text{tot,dis}}$	sumAs	$A_{\text{tot,dis}}$	sumAs	$A_{\text{tot,dis}}$	sumAs
SN	1.10	1.03	1.14	1.11	1.38	1.29
S1	1.98	1.93	5.95	5.87	9.52	10.4
S2	3.31	3.23	17.3	17.3	9.02	8.75
S3	4.41	4.38	9.01	8.94	4.06	3.74

Table SI12. iAs(III+V) and iAs(III) concentrations (ng L<sup>-1</sup>) determined by HG-CT-ICP-MS at 10 depths and 6 sampling dates at GE3.

	26 January 2021		16 February 2021		16 March 2021		20 April 2021		15 May 2021		22 June 2021	
Depth/ m	iAs(III+V)	iAs(III)	iAs(III+V)	iAs(III)	iAs(III+V)	iAs(III)	iAs(III+V)	iAs(III)	iAs(III+V)	iAs(III)	iAs(III+V)	iAs(III)
0	847	23.5	841	23.7	718	61.5	744	341	787	238	591	253
2.5	838	22.6	845	24.1	711	65.6	743	385	792	240	598	272
5	844	23.5	846	24.5	715	68.2	754	399	800	240	599	250
7.5	850	23.5	849	24.4	713	68	745	418	783	236	642	252
10	843	23	849	23.8	719	67.8	744	399	794	217	662	272
15	858	22.5	845	24.2	715	67.1	746	283	799	182	747	354
20	850	22.5	839	24.5	722	62.7	744	225	806	188	763	235
30	863	23	838	24.5	717	66.1	749	187	838	67.5	786	48.4
50	864	22.8	839	25	716	65.6	773	134	895	39.9	910	38.7
65	866	22.6	824	25.3	716	64.9	796	89.2	944	30.9	964	28.1

Table SI13. MA(III+V), DMA(III+V) and TMAO concentrations (ng L<sup>-1</sup>) determined by HG-CT-ICP-MS at 10 depths and 6 sampling dates at GE3.

Depth/ m	26 January 2021			16 February 2021			16 March 2021			20 April 2021			15 May 2021			22 June 2021		
	MA(III+V)	DMA(III+V)	TMAO	MA(III+V)	DMA(III+V)	TMAO	MA(III+V)	DMA(III+V)	TMAO	MA(III+V)	DMA(III+V)	TMAO	MA(III+V)	DMA(III+V)	TMAO	MA(III+V)	DMA(III+V)	TMAO
0	10.3	10.4	20.8	8.6	11.7	20.2	7.5	39.6	17.5	11.2	103	18.1	18.1	56.7	19.9	27.9	205.2	23.4
2.5	10.2	10.3	21	8.5	11.6	20.4	7.4	39.5	17.7	10.9	103	17.7	18.1	57.1	19.7	27.7	198.7	23.5
5	10.2	10.6	21.2	8.5	12.3	20.3	7.4	39.6	17.8	10.9	102	18.4	18.1	57.1	20.1	26.8	197.1	23.7
7.5	10.4	10.6	21	8.6	11.6	20.5	7.4	39.1	17.5	10.9	103	18.1	17.8	55	19.7	26.7	183	23.4
10	10.6	10.4	20.6	8.7	11.8	20.3	7.4	39.2	17.2	10.6	102	17.8	17.7	53.4	19.9	26.2	158.6	23.6
15	10.4	10.4	20.9	8.6	11.8	20.5	7.5	40	17.4	10.4	100	17.4	16.6	47.3	19.2	22.8	85.3	22.9
20	10.2	10.5	20.7	8.5	11.6	20.4	7.1	40.8	16.7	10.5	98	17.9	16.7	48.3	19.1	18.6	56.4	22.3
30	10.6	10.7	21.2	8.5	11.8	20.6	7.4	38.3	17.2	10.4	97.9	17.7	12.7	27	17.8	12.1	28.2	20.8
50	10.6	10.9	20.8	8.5	11.8	20.3	7.3	37.7	17.2	10.3	90.1	17.4	8.3	25.5	15.9	8.6	28.1	16
65	10.8	11.5	21	8.1	11.8	20.2	7.4	37.7	17.4	9.3	73.4	16.8	5.4	24.4	14.1	5.2	23.8	13.6

Table SI14. iAs(III+V), iAs(III) MA(III+V), DMA(III+V) and TMAO concentrations (ng L<sup>-1</sup>) determined by HG-CT-ICP-MS at two sampling dates and 11 and 13 depths, respectively, at SHL2.

Depth / m	20 April 2021					14 June 2021				
	iAs(III+V)	iAs(III)	MA(III+V)	DMA(III+V)	TMAO	iAs(III+V)	iAs(III)	MA(III+V)	DMA(III+V)	TMAO
0	737	322	9.7	103	19.5	621	320	24.6	175	23.2
5	723	328	10	104	18.3	681	304	25	124	22.6
10	720	392	9.6	102	19.3	740	283	19.6	59.8	22
15	716	276	9.6	101	19.1	643	114	13.6	40	21.1
20						740	73.3	11.5	30	20.6
25						847	38.3	9.8	24.2	17.5
30	735	237	9.4	96.1	18	839	33.9	9.9	22.8	17.9
35	790	124	7.4	58.7	18.1	895	21.6	8.5	22	16.5
50	857	26.7	5.2	31.7	17.1	904	16.8	7.1	20	15.4
100	890	9.3	3.5	17.5	13.8	952	11.7	3.4	16.3	12.3
150	1151	8.5	1.4	14.6	5.1	1235	8.3	1.5	15.9	4.8
200	1459	8.2	0.7	14.7	1.5	1510	9.1	1	15.5	1.7
300	1965	9	1.2	13.3	1.8	2008	8.5	1.7	18.3	1.8

Table SI15. iAs(III+V), iAs(III) MA(III+V), DMA(III+V) and TMAO concentrations (ng L<sup>-1</sup>) in three sediment cores (C1, C2, C3). See text for location. SN: supernatant, S1: 1 cm, S2: 4 cm, S3: 7 cm under the sediment-water interface, 12 July 2021.

	C1					C2					C3				
	iAs(III+V)	iAs(III)	MA(III+V)	DMA(III+V)	TMAO	iAs(III+V)	iAs(III)	MA(III+V)	DMA(III+V)	TMAO	iAs(III+V)	iAs(III)	MA(III+V)	DMA(III+V)	TMAO
SN	991	29	5.7	21.9	14.1	1007	35	6.8	79	14.5	1209	185	6.2	62.4	13.1
S1	1913	1600	4.6	13.3	1	5806	4315	6.6	46.5	9.1	10290	7905	8.7	52.4	6.6
S2	3215	2494	6	9.7	1.3	17230	14115	12.7	35.6	2.1	8704	6885	10.6	34.2	1.4
S3	4357	3275	8.1	10.7	1.2	8899	6846	18.1	25.2	1.3	3694	2649	8.6	33.9	0.4

Table SI16a. Seasonality analysis. Results of Kruskal-Wallis test ( $p$  values) for each period and all data normalised. Period 2 is excluded because of the analytical issues discussed in the text. Values in bold are significant.

Depth / m	Instrument			All data after normalisation
	Period 1	Period 2	Period 3	
0	0.1	excluded	<b>0.00726</b>	<b>0.0188</b>
2.5	<b>0.037</b>	excluded	<b>0.0186</b>	<b>1.39 x 10<sup>-3</sup></b>
5	<b>0.00696</b>	excluded	<b>0.0104</b>	<b>2.92 x 10<sup>-4</sup></b>
7.5	<b>0.00696</b>	excluded	<b>0.0242</b>	<b>4.60 x 10<sup>-3</sup></b>
10	0.0681	excluded	<b>0.00235</b>	<b>6.98 x 10<sup>-4</sup></b>
15	0.563	excluded	<b>0.0126</b>	0.0854
20	0.364	excluded	0.381	0.149
30	0.804	excluded	0.991	0.774
50	0.386	excluded	0.441	0.189
70 <sup>a</sup>	0.466	excluded	0.299	0.116
All depths				<b>9.73 x 10<sup>-22</sup></b>

<sup>a</sup>2021 values measured at 65 m.

Table SI16b. Seasonality analysis. Results of Kruskal-Wallis test (*p* values) for each period and all data normalised. Values in bold are significant.

Depth / m	Instrument			All data after normalisation
	Period 1	Period 2	Period 3	
0	0.1	<b>0.0176</b>	<b>0.00726</b>	<b>1.19 x 10<sup>-5</sup></b>
2.5	<b>0.037</b>	<b>0.0231</b>	<b>0.0186</b>	<b>1.17 x 10<sup>-5</sup></b>
5	<b>0.00696</b>	<b>0.0289</b>	<b>0.0104</b>	<b>1.43 x 10<sup>-8</sup></b>
7.5	<b>0.00696</b>	0.0623	<b>0.0242</b>	<b>2.14 x 10<sup>-6</sup></b>
10	0.0681	0.0537	<b>0.00235</b>	<b>8.15 x 10<sup>-7</sup></b>
15	0.563	0.0989	<b>0.0126</b>	<b>3.89 x 10<sup>-4</sup></b>
20	0.364	0.185	0.381	<b>0.0110</b>
30	0.804	0.504	0.991	0.190
50	0.386	0.276	0.441	<b>0.00797</b>
70 <sup>a</sup>	0.466	0.0809	0.299	<b>0.00604</b>
All depths				<b>1.10 x 10<sup>-31</sup></b>

<sup>a</sup>2021 values measured at 65 m.

Table SI7a. Temporal trend analysis. Results of the seasonal Mann-Kendall test (SMK) for each period and all data normalised. Period 2 is excluded because of the analytical issues discussed in the text. No value is significant ( $p < 0.05$ ).

	SMK Z
Period 1	-1.33
Period 2	excluded
Period 3	1.22
All data after normalization	0.725

Table SI7b. Temporal trend analysis. Results of the seasonal Mann-Kendall test (SMK) for each period and all data normalised. No value is significant ( $p < 0.05$ ).

	SMK Z
Period 1	-1.33
Period 2	-0.013
Period 3	1.22
All data after normalization	0.232

Figure S11. Water discharge of the River Rhone at « Porte-du-Scex ». Values cover the period 1935–2021. Black arrows point to our two sampling dates. Source: [www.hydrodaten.admin.ch/](http://www.hydrodaten.admin.ch/).

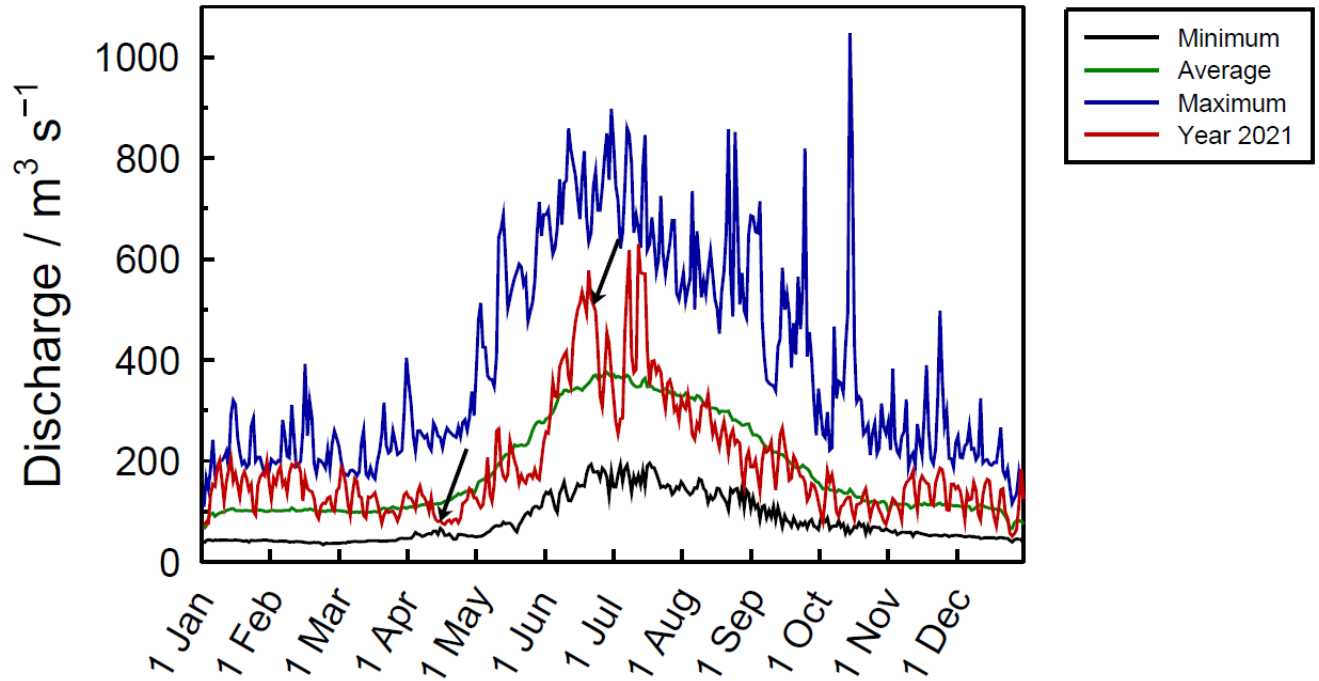


Figure SI2. Pore water sampling using Rhizon Core Solution Sampler. Sampling depths are indicated with arrows. SN: supernatant, S1: 1 cm, S2: 4 cm, S3: 7 cm under the sediment-water interface.

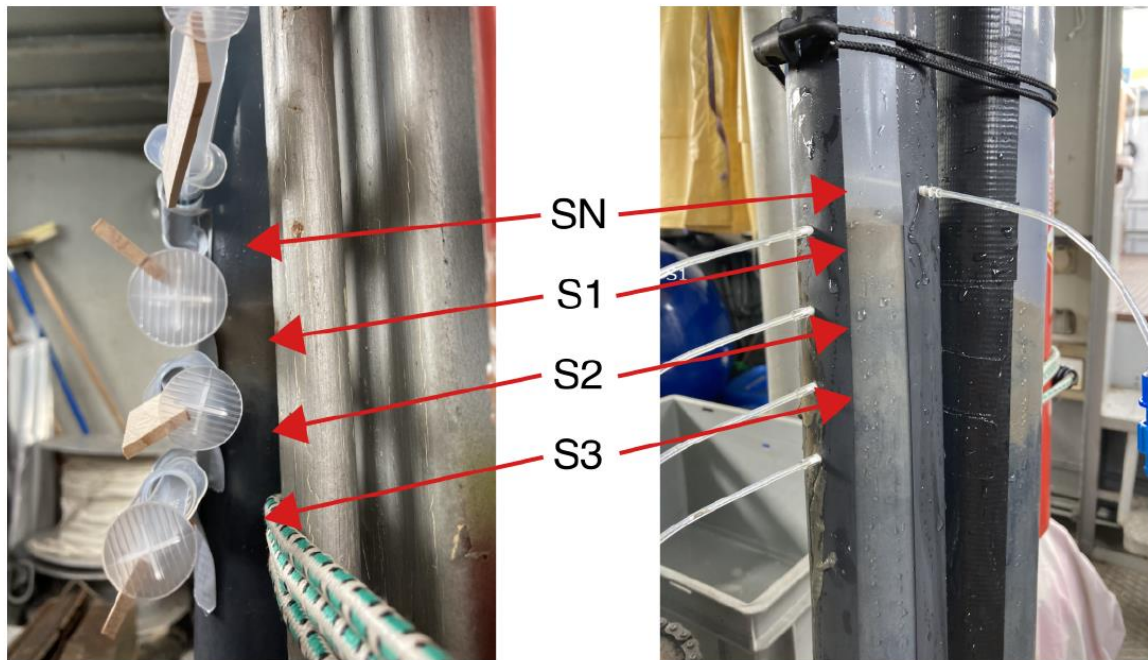


Figure SI3. Monthly specific As mass inventories of  $A_{Stot,dis}$  from 2015 to 2021. See definition in text. Different colours have no particular meaning, they are just used to improve figure readability (corresponding axes have the same colour).

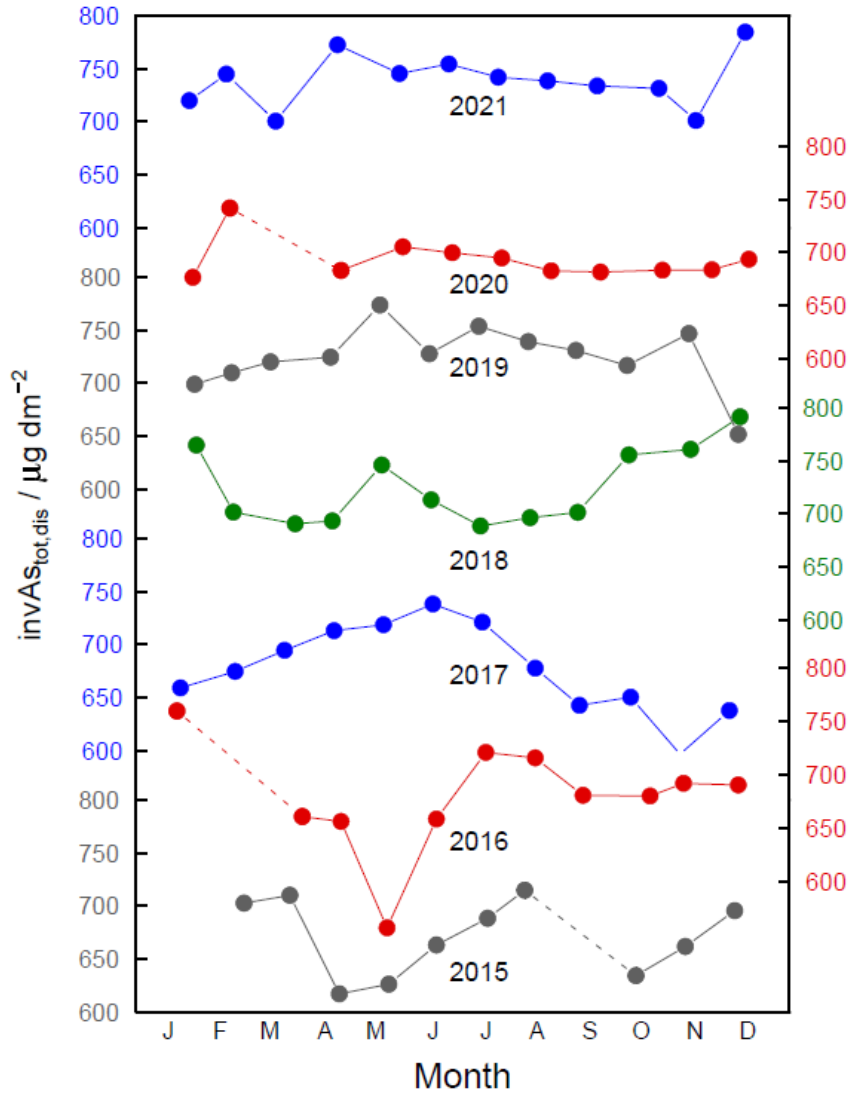
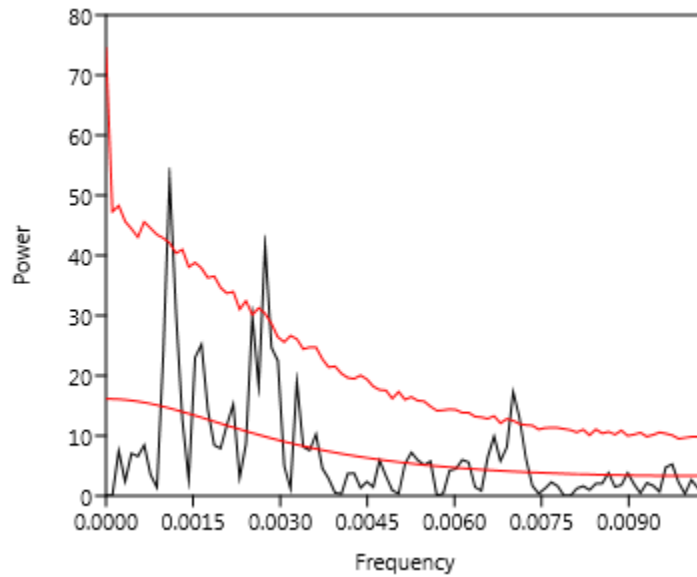


Figure SI4. Fourier power spectra (REDFIT) of normalized total ‘dissolved’ As concentrations at 0 and 70 m at point G3. Period 2 of analysis has been excluded. Peaks above the irregular upper red line 95 % confidence level of AR(1) noise spectral power (represented with the regular inferior red line) are thus significant at 95% confidence level (calculated with 1,000 Monte Carlo runs). The annual peak is at a frequency of  $0.00274 \text{ day}^{-1}$  and clearly stands above the 95% level of AR(1) spectral power at 0 m, but is below that line at 70 m, in agreement with the seasonality results (Table SI16a).

0 m



70 m

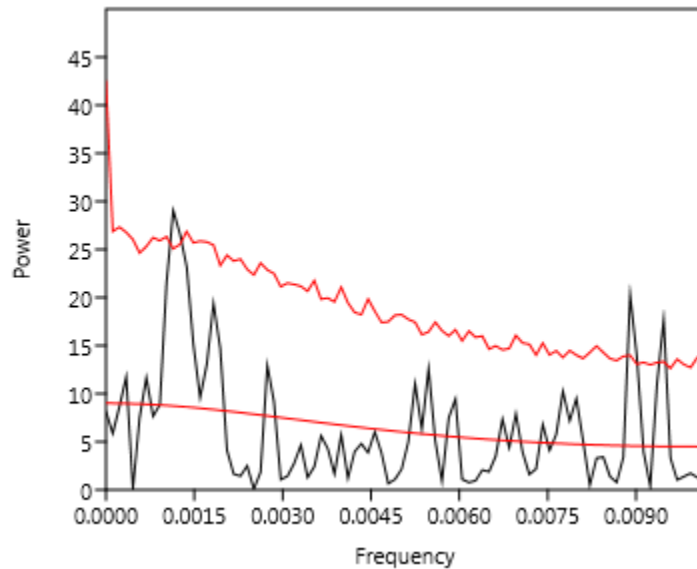
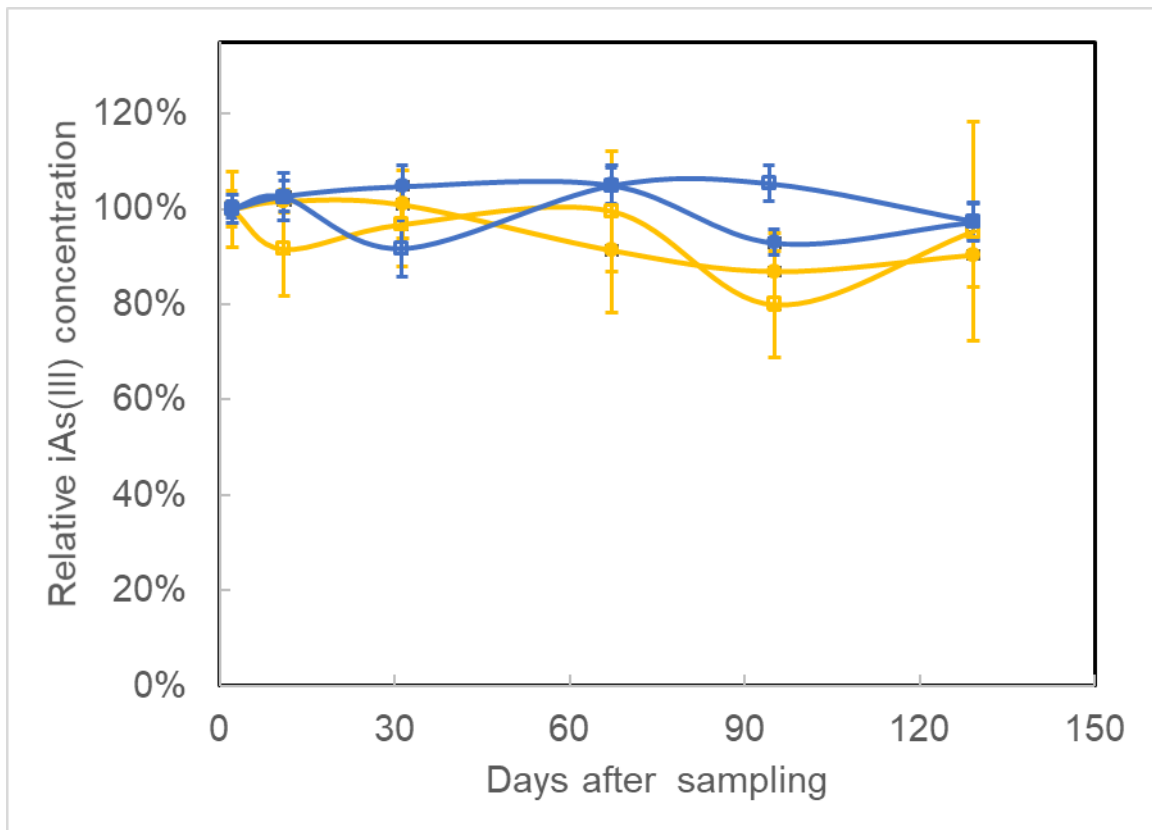


Figure SI5. Stability of iAs(III) species in lake water. Full squares- natural concentration; empty squares: spiked with 500 ng L<sup>-1</sup> iAs(III); blue: stabilized with 2 mM EDTA; yellow: stabilized with HNO<sub>3</sub> to pH 1.



## References

- 1 T. Matoušek, J. M. Currier, N. Trojánková, J. R. Saunders, M. C. Ishida, C. Gonzalez-Horta, S. Musil, Z. Mester, M. Stýblo and J. Dědina, Selective hydride generation – cryotrapping – ICP-MS for arsenic speciation analysis at picogram levels: analysis of river and sea water reference materials and human bladder epithelial cells, *J. Anal. At. Spec.*, 2013, **28**, 1456–1465. doi:10.1039/c3ja50021g
- 2 M. Filella and T. Matoušek, Germanium in Lake Geneva (Switzerland/France) along the spring productivity period, *Appl. Geochem.*, 2022, **143**, 105352. doi:10.1016/j.apgeochem.2022.105352
- 3 A. García-Figueroa, M. Filella and T. Matoušek, Speciation of germanium in environmental water reference materials by Hydride Generation and Cryotrapping in combination with ICP-MS/MS, *Talanta*, 2021, **225**, 121972. doi:10.1016/j.talanta.2020.121972
- 4 T. Matoušek, A. Hernandez-Zavala, M. Svoboda, L. Langerová, B. M. Adair, Z. Drobná, D. J. Thomas, M. Stýblo and J. Dědina, Oxidation state specific generation of arsines from methylated arsenicals based on L-cysteine treatment in buffered media for speciation analysis by hydride generation-automated cryotrapping-gas chromatography-atomic absorption spectrometry with the multiatomizer, *Spectrochim. Acta B: At. Spec.*, 2008, **63**, 396–406. doi:10.1016/j.sab.2007.11.0370
- 4 K. A. Francesconi and D. Kuehnelt, Determination of arsenic species: A critical review of methods and applications, 2000-2003, *Analyst*, 2004, **129**, 373–395. doi:10.1039/B401321M
- 5 CIPEL, *Rapports sur les Études et Recherches Entreprises dans le Bassin Lémanique Campagne 2021*, CIPEL: Nyon, Switzerland. 2022. [www.cipel.org/wp-content/uploads/2022/11/rapport-scientifique-2021-2022-low.pdf](http://www.cipel.org/wp-content/uploads/2022/11/rapport-scientifique-2021-2022-low.pdf). Last accessed: 2 January 2023.